

Low-lying unoccupied electronic states in 3*d* transition-metal fluorides probed by NEXAFS at the F 1*s* threshold

A. S. Vinogradov,^{1,*} S. I. Fedoseenko,¹ S. A. Krasnikov,^{1,2} A. B. Preobrajenski,^{1,3} V. N. Sivkov,¹ D. V. Vyalikh,^{1,4,5} S. L. Molodtsov,^{1,4,5} V. K. Adamchuk,¹ C. Laubschat,⁵ and G. Kaindl⁶

¹*V.A. Fock Institute of Physics, St. Petersburg State University, 198504 St. Petersburg, Russia*

²*W. Ostwald-Institut für Physikalische und Theoretische Chemie, Universität Leipzig, D-04103 Leipzig, Germany*

³*MAX-lab, Lund University, S-22100 Lund, Sweden*

⁴*Russian-German Laboratory at BESSY, D-12489 Berlin-Adlershof, Germany*

⁵*Institut für Festkörperphysik, Technische Universität Dresden, D-01062 Dresden, Germany*

⁶*Institut für Experimentalphysik, Freie Universität Berlin, D-14195 Berlin, Germany*

(Received 5 July 2004; revised manuscript received 22 October 2004; published 27 January 2005)

The near-edge x-ray absorption fine structure (NEXAFS) at the F 1*s* threshold has been studied with high-energy resolution for a series of binary fluorides, including KF, TiF₄, VF₄, VF₃, CrF₃, CrF₂, MnF₃, MnF₂, FeF₃, FeF₂, CoF₂, NiF₂, CuF₂, and ZnF₂ as well as for SF₆ in the gas phase, and for the PF₆[−] and TiF₆^{2−} molecular anions of the solid compounds KPF₆ and K₂TiF₆. Most of these spectra were measured at the Russian-German beamline at BESSY II, while the spectra of KF and CuF₂ were taken under comparable experimental conditions at the D1011 beamline at MAX-lab. The spectra of the solid samples were recorded via the total electron yield. The NEXAFS spectra were taken with the aim to elucidate the role of covalent bonding and its manifestation in x-ray absorption spectra as well as to gain information on the electronic structure of the conduction band along the whole series of 3*d* transition-metal (TM) fluorides. The spectra of these most ionic compounds of the 3*d* TM's have been analyzed in a comparative way considering also the F 1*s* NEXAFS spectrum of the molecular TiF₆^{2−} anion in solid K₂TiF₆. In its turn, the latter spectrum has been interpreted by comparing with the F 1*s* NEXAFS spectrum of the molecular PF₆[−] anion in KPF₆ and that of SF₆ in the gas phase. In this way, the low-lying empty electronic states of the 3*d* TM fluorides are shown to be formed by covalent mixing of the TM 3*d* with the fluorine 2*p* electronic states. It is further found that the number of low-lying empty electronic states with TM 3*d*–fluorine 2*p* hybridized character decreases gradually along the series of 3*d* TM fluorides, and is essentially zero in the case of ZnF₂.

DOI: 10.1103/PhysRevB.71.045127

PACS number(s): 71.20.–b, 71.70.Ch, 78.70.Dm

I. INTRODUCTION

The great variety of properties observed in 3*d* transition-metal (TM) compounds is commonly related to the different role of correlation effects between strongly localized 3*d* electrons, charge fluctuations, and covalent bonding between the 3*d* TM atoms and the neighboring atoms in various compounds.¹ Until recently, the 3*d* electron correlation has been considered to be dominant in the electronic structure of most 3*d* TM compounds. At the same time it is apparent that the TM 3*d* electrons can participate in covalent bonding to an extent that will strongly depend on the electronic structure of the ligands. This covalent mixing (hybridization) between the TM 3*d* electrons and ligand valence electrons leads to a delocalization of the 3*d* states, and hence to a decrease of the 3*d* electron density at the TM atoms and—as a consequence—to a weakening of the 3*d* electron correlation. The subtle interplay between hybridization and 3*d* correlation in the electronic structure can be accounted for by a systematic comparative investigation of a variety of different TM compounds using modern x-ray spectroscopic techniques, in particular high-resolution x-ray absorption fine-structure (NEXAFS) spectroscopy, which has become a powerful tool for probing empty electronic states. Although NEXAFS spectroscopy has been widely used for more than two decades to gain information on the energy distribution

and spatial localization of unoccupied electronic states in 3*d* TM compounds, a systematic study of the role of hybridization in the formation of the electronic structure of these compounds is still missing.

This work presents F 1*s* NEXAFS spectra recorded with high-energy resolution for a series of binary fluorides, including TiF₄, VF₄, VF₃, CrF₃, CrF₂, MnF₃, MnF₂, FeF₃, FeF₂, CoF₂, NiF₂, CuF₂, and ZnF₂. The NEXAFS spectra were measured with the aim to elucidate the role of covalent bonding and its manifestation in NEXAFS spectra as well as to gain information on the electronic structure of the conduction band along the whole series of 3*d* TM compounds. We chose the 3*d* TM fluorides for this study since they are the most ionic and simplest ones among the 3*d* TM compounds. It is expected that the spectra of these TM fluorides together with the derived electronic-structure information provide the basis for an improved understanding of the electronic properties of more complicated and also more covalent compounds. Since in most of these compounds the 3*d* atoms are coordinated octahedrally or almost octahedrally to fluorine atoms, a possible covalent bonding between the TM and the surrounding atoms can be realized within the MF₆ structural group. In the context of a simple ionic model, which has been mainly used up to now, it is quite natural to assume that a covalent TM 3*d*–F 2*p* bonding in the fluorides is virtually absent, so that the lower conduction band of the TM fluo-

rides is formed solely by $3d$ states of the positive TM ions. On the basis of a comparative analysis of the F $1s$ NEXAFS spectra of TM fluorides and of isostructural (octahedral) covalent systems (SF_6 molecule as well as PF_6^- and TiF_6^{2-} molecular anions) we shall show that this is not correct. Even in the case of such strongly ionic compounds of the $3d$ TM's as fluorides, covalent bonding plays an important role, causing a mixed TM $3d$ -F $2p$ character of the empty electronic states near the bottom of the conduction band.

II. EXPERIMENT

We studied near-edge x-ray absorption fine-structure (NEXAFS) spectra at the F $1s$ threshold of binary fluorides in the solid phase, including KF, TiF_4 , VF_4 , VF_3 , CrF_3 , CrF_2 , MnF_3 , MnF_2 , FeF_3 , FeF_2 , CoF_2 , NiF_2 , CuF_2 , and ZnF_2 , of SF_6 in the gas phase, and of the PF_6^- and TiF_6^{2-} molecular anions of the solid compounds KPF_6 and K_2TiF_6 . The $2p$ absorption spectra of titanium for TiF_6^{2-} , TiF_4 , TiO_2 , and of potassium for KF were investigated additionally in order to facilitate the interpretation of the F $1s$ absorption structures in the spectra of titanium and potassium fluorides. Most of these spectra were recorded at the Russian-German beamline operated at the Berliner Elektronenspeicherring für Synchrotronstrahlung (BESSY II),²⁻⁴ while the spectra of KF and CuF_2 were taken under similar experimental conditions at the D1011 beamline of MAX-lab, Lund, Sweden. All materials were obtained commercially and were studied without further purification. The spectra of the solid materials were obtained by monitoring the total electron yield from samples that were prepared by rubbing powders of solid materials into the scratched surface of a clean copper plate. No noticeable charging effects were observed in the experiments. The NEXAFS spectra of SF_6 and Ne in the gas phase were measured by detecting the total photoionization yield with the help of a gas cell with an entrance window made of a thin aluminum foil. The resolving power $E/\Delta E$ exceeded 6000 for the energy range up to 870 eV, as estimated from the analysis of the linewidth of the first separated $1s \rightarrow 3p$ line in the absorption spectrum of gas-phase Ne. This line was fitted by a combination of Lorentzian and Gaussian line shapes with half widths of 305 and 144 meV, respectively. The Lorentzian and Gaussian half widths simulate the line shape due to the natural width of the Ne $1s$ level and the instrumental function of the monochromator, respectively.⁵ As estimated from these data, the energy resolution of the monochromator ΔE in the range of the F $1s$ absorption threshold ($h\nu \cong 690$ eV) was approximately 115 meV. The absorption spectra were normalized to the incident photon flux, which was monitored by detecting the photocurrent from a gold mesh placed at the outlet of the beamline. The photon energy in the region of the F $1s$ absorption spectrum was calibrated using the known position (683.9 eV) of the first narrow peak in the F $1s$ absorption spectrum of K_2TiF_6 ,⁶ which was recorded before and after each measurement of a fluoride spectrum.

III. RESULTS AND DISCUSSION

A. Overview

The F $1s$ NEXAFS spectra of the TM fluorides studied in this work over the photon-energy range from 675 to 760 eV

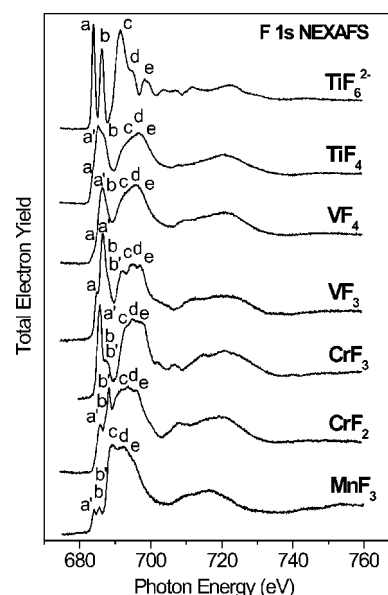


FIG. 1. F $1s$ NEXAFS spectra of the $3d$ TM fluorides K_2TiF_6 , TiF_4 , VF_4 , VF_3 , CrF_3 , CrF_2 , and MnF_3 . The spectra were normalized to the same continuum jump at 760 eV.

are presented in Figs. 1 and 2; the labeled NEXAFS features are discussed below. For the majority of the studied binary TM fluorides, these high-resolution F $1s$ spectra were obtained. Previously, only the spectra of some TM difluorides,⁷ and of ScF_3 (Ref. 8) had been reported with lower resolution. The F $1s$ NEXAFS spectra of the TiF_6^{2-} and PF_6^- anions in solid K_2TiF_6 and KPF_6 , respectively, shown in Fig. 3, exhibit a fine structure similar to that previously reported,^{6,9} but with much better resolution. For SF_6 in the gas phase, the line shapes and energy positions of the spectral structures in the

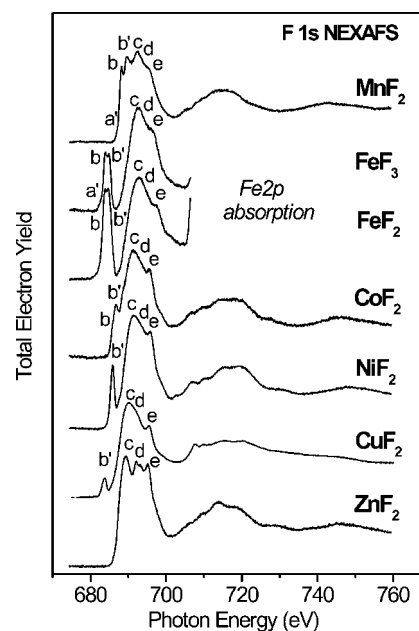


FIG. 2. F $1s$ NEXAFS spectra of the $3d$ TM fluorides MnF_2 , FeF_3 , FeF_2 , CoF_2 , NiF_2 , CuF_2 , and ZnF_2 . The spectra were normalized to the same continuum jump at 760 eV.

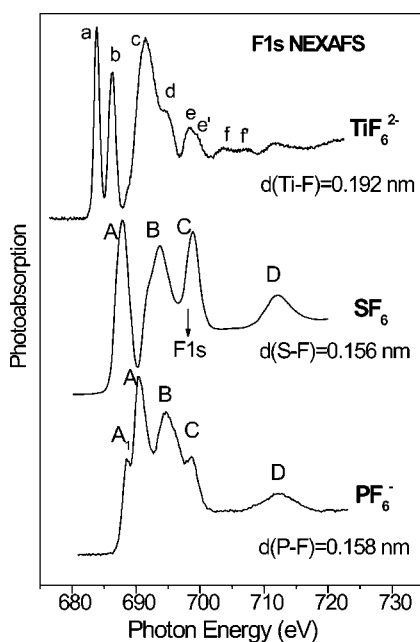


FIG. 3. F 1s NEXAFS spectra of the covalent anions TiF_6^{2-} and PF_6^- in solid K_2TiF_6 and KPF_6 as well as of SF_6 in the gas phase. The vertical arrow indicates the energy of the F 1s ionization threshold for the molecule [695.04 eV (Ref. 22)].

F 1s NEXAFS spectrum, presented also in Fig. 3, correlate again well with the spectra that had previously been reported.^{10–14} The same is true for the F 1s spectrum of KF, presented in Fig. 8, which compares well with spectra reported in the literature.^{15,16} Some of the spectra presented in this work had been briefly discussed before.¹⁷ Finally, it should be emphasized that the spectra presented here are of particular interest because they were measured under the same experimental conditions, thus allowing us to discuss changes in x-ray absorption spectra and electronic structure along the entire series of 3d TM fluorides.

The NEXAFS spectra of the TM fluorides in Figs. 1 and 2 were normalized to equal absorption edge jumps. The spectra are quite different from that of K_2TiF_6 and they show substantial variations along the series of 3d TM fluorides (with increasing number of 3d electrons). Nevertheless, one can distinguish three spectral regions, where the spectral features are similar in all spectra, including that of covalent TiF_6^{2-} . The first region contains the narrow resonances a , a' , b , and b' , located below the F 1s absorption threshold (at ~ 690 eV). The second region is dominated by the broader absorption bands c , d , and e that are located slightly above the absorption threshold and overlap significantly with each other. It should be noted that the F 1s NEXAFS spectrum of ScF_3 reported in Ref. 8, despite a lower energy resolution, contains also two similar regions. The third energy region (above ~ 705 eV) displays rather broad and less intensive EXAFS-like oscillations.

Since for all of the studied fluorides an octahedral or nearly octahedral coordination of the 3d atoms by fluorine is typical, these crystals are commonly considered as three-dimensional arrays of interlinked distorted MF_6 octahedra.¹⁸ In this case, covalent bonding between the 3d TM atom M

and the surrounding fluorine can take place within the octahedron due to a mixing of the valence M 3d, 4s, 4p, and F 2p electronic states. In order to learn how such a hybridization of the valence states can manifest itself in the F 1s NEXAFS spectra of binary TM fluorides, we first consider the origin of the absorption features in the spectra of the covalent molecular TiF_6^{2-} anion in solid K_2TiF_6 .

B. Assignment of absorption features for the covalent molecular TiF_6^{2-} anion

In Fig. 3 we compare the F 1s NEXAFS spectra of the following isostructural covalent molecules: SF_6 in the gas phase and the solid-state molecular anions PF_6^- and TiF_6^{2-} , representing isolated regular octahedra.¹⁸ The spectrum of SF_6 exhibits a well-developed fine structure with peaks labeled A–D that result from the F 1s electron transitions to unoccupied molecular orbitals (MO's) of a_{1g} , t_{1u} , t_{2g} , and e_g symmetry.^{10–14,19–21} The excited molecular states formed in this case are often considered as molecular shape resonances, underlining in this way their fundamental relationship with quasistationary states (shape resonances), that prevail in the resonance (multiple) scattering of low-energy (photo)electrons by a molecular potential.^{19–21} Transitions to unoccupied MO's of a_{1g} and t_{1u} symmetry (formed from the S 3s and 3p orbitals with an admixture of F 2p orbitals) are responsible for the absorption peaks A and B below the F 1s ionization threshold in SF_6 [695.04 eV (Ref. 22)]. The features C and D appear in the continuum significantly above the threshold resulting from transitions to the MO's t_{2g} and e_g . These MO's are formed by covalent mixing of the S 3d with the F 2p states, so that the corresponding peaks can be observed in the absorption spectra of both sulfur and fluorine at almost the same energy positions above the vacuum level.^{10–14} Since the contributions from S 3d orbitals dominate in the MO's t_{2g} and e_g , the energy positions of bands C and D relative to the F 1s ionization threshold reflect actually the energies of S 3d states relative to the vacuum level, which are split into $3dt_{2g}$ and $3de_g$ components in the anisotropic field of the fluorine octahedron. This ligand-field splitting of the 3d states in the MF_6 octahedron ($10Dq$) is given by $10Dq = 5eq\langle r^4 \rangle_{3d} / 3R^5$, where q is the charge on each ligand atom (fluorine), $\langle r^4 \rangle_{3d}$ is the expectation value of the operator r^4 for the TM 3d wave function, and R is the interatomic distance $R(M-F)$.^{23–25} $10Dq$ is equal to 13.3 eV in the F 1s absorption spectrum of the SF_6 molecule.^{10–14}

It should be noted that unoccupied electronic states (MO's) of SF_6 observed in the F 1s absorption spectrum are somewhat disturbed by the F 1s core hole. This final-state effect is well known and quantitatively evaluated for polyatomic molecules like SF_6 on the basis of comparison between their x-ray or UV absorption spectra (with a core hole) and electron-molecule scattering spectra (without it).^{19–21} Primarily, the core hole is responsible for certain low-energy shifts in the energy positions of the localized unoccupied MO's. On the other hand, the ordering of low-energy unoccupied electronic states is retained, and relative energy separations between them do not change significantly.^{19–21} Evidently, such behavior of empty electronic states indicates that

the changes caused by a core hole in the atomic-orbital composition of unoccupied MO's are rather small. We assume that the same is qualitatively valid not only for molecules, but also for quasimolecular groups in solids. In particular, it should be valid for the MF_6 quasimolecules in $3d$ TM fluorides. Thus, considering below covalent bonding effects in the F $1s$ NEXAFS spectra of these fluorides, we will assume that the F $1s$ hole shifts the positions of all unoccupied MO's to lower energies by more or less the same value, and its influence on the degree of the $M 3d-F 2p$ hybridization is not large.

Figure 3 provides evidence for a strong similarity between the F $1s$ NEXAFS spectrum of the SF_6 molecule and that of the PF_6^- molecular anion in solid KPF_6 , which is actually not surprising. Indeed, the PF_6^- anion is a separate structural unit of the crystal with essentially covalent bonds between the phosphorus and fluorine atoms; it is an isostructural and isoelectronic analog of the SF_6 molecule. These facts, along with the rather similar interatomic distances in these polyatomic systems [$R(S-F)=0.156$ nm and $R(P-F)=0.158$ nm (Ref. 18)], explain the similarity between the fine structures observed in the spectra of the molecule and of the solid molecular anion, including the very similar $3d$ splitting in SF_6 (13.3 eV) and PF_6^- (13.6 eV). Indeed, the above expression for the crystal-field splitting gives closely related energy separations between the $3dt_{2g}$ and $3de_g$ components for these polyatomic molecules, since their interatomic distances $R(M-F)$ are essentially equal and $\langle r^4 \rangle_{3d}$ decreases only slightly when going from the P to the S atom. It is thus possible to relate bands C and D in the F $1s$ spectrum of PF_6^- (as in the case of SF_6) to the $3d$ states of the central atom (phosphorus) and to use their energies relative to the F $1s$ ionization threshold for estimating the energy positions of these states relative to the vacuum level (see further below).

In the spectra of unoccupied electronic states in the hexafluorides of phosphorus and sulfur, the $3d$ states of the central atom appear only in the continuum. These states can be probed by x-ray absorption on both the P(S) and F sites. It is of interest to find out whether the F $1s$ absorption spectra can also be used to probe $3d$ states in the first-row TM fluorides, where the $3d$ shell is only partly filled. We anticipate that this will only be possible if the covalent bonding between the $3d$ TM atom and the fluorine atoms is sufficiently strong. With this in mind, we first consider the F $1s$ NEXAFS spectrum of the covalent molecular anions TiF_6^{2-} in crystalline K_2TiF_6 (see Fig. 3), using the spectra of SF_6 and PF_6^- as references. While the F $1s$ NEXAFS spectra of SF_6 and PF_6^- are quite similar, they differ considerably from the spectrum of TiF_6^{2-} , where the resonances C and D are missing, while two rather narrow and intense absorption peaks *a* and *b* show up in the low-energy spectral region; in addition, the onset of the F $1s$ absorption is shifted to lower energies by several eV. It is remarkable that the widths (FWHM, full width at half maximum) of peaks *a* and *b* in the spectrum of solid K_2TiF_6 (FWHM ≈ 1 eV) are significantly smaller than the width of the lowest-energy peak A in the spectrum of gas phase SF_6 (FWHM ≈ 2.3 eV).

In order to obtain further insight in the origin of these narrow peaks, we studied additionally the Ti $2p$ absorption

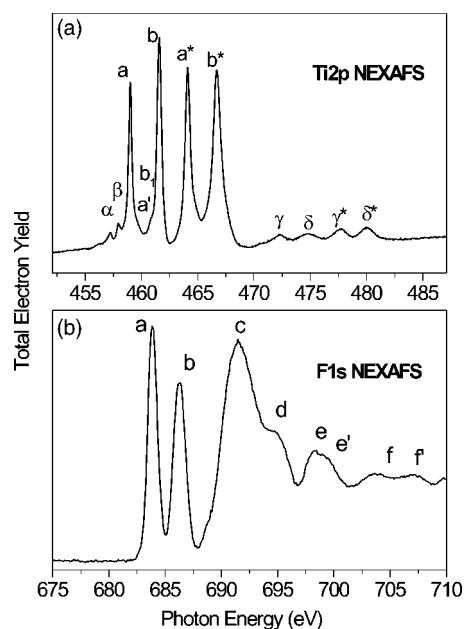


FIG. 4. Ti $2p_{1/2,3/2}$ (a) and F $1s$ (b) NEXAFS spectra of the molecular anion TiF_6^{2-} in solid K_2TiF_6 . The Ti $2p_{1/2}$ structures were labeled by letters with asterisks. The spectra are aligned in energy using the measured energy separation (222.9 eV) between the F $1s$ and Ti $2p_{3/2}$ core levels of K_2TiF_6 .

spectrum in K_2TiF_6 (see Fig. 4). This spectrum should reflect the energies of the free $3d$ states in the most direct way, because it is dominated by the $2p \rightarrow 3d$ dipole transitions in the Ti atoms.^{26,27} The absorption Ti $2p$ spectrum was measured with an energy resolution of ≈ 75 meV (FWHM), and reflects clearly the spin-orbit splitting of the Ti $2p$ level. The energy separation between the $2p_{3/2}$ and $2p_{1/2}$ components (the latter marked by an asterisk in Fig. 4) is close to 5.2 eV, i.e., equal to the spin-orbit splitting of the Ti $2p$ level in TiF_4 .²⁸ In Fig. 4, the Ti $2p$ spectrum was aligned in energy to the F $1s$ spectrum using the energy difference of 222.9 eV between the F $1s$ and Ti $2p_{3/2}$ levels of K_2TiF_6 . This splitting was obtained with an Escalab 220iXL spectrometer at the Wilhelm-Ostwald-Institute, Leipzig, using monochromatized Al $K\alpha$ radiation; it coincides with that reported in Ref. 6. The narrow and intense peaks *a* and *b* in the Ti $2p_{3/2}$ spectrum stem from dipole-allowed transitions of Ti $2p_{3/2}$ electrons to unoccupied $3d$ states. Similar to the case of PF_6^- and SF_6 , these states are split into $3dt_{2g}$ (peak *a*) and $3de_g$ (peak *b*) components by the octahedral crystal field created by the fluorine ions. These peaks in the Ti $2p$ spectrum correspond (with respect to lineshape and energy position) to the low-energy peaks *a* and *b* in the F $1s$ NEXAFS spectrum. It is reasonable to assume that these peaks are of the same nature reflecting transitions of core electrons of Ti and F to the molecular states t_{2g} and e_g of the TiF_6^{2-} anion, with strong covalent Ti $3d-F 2p$ mixing in both cases. The small differences (less than 2 eV) in the energy positions of these states observed in the spectra of Ti and F may naturally be attributed to a different impact of the F $1s$ and Ti $2p_{3/2}$ core holes on the states under consideration. This final-state effect occurs mainly due to Coulomb and exchange interaction between an inner-shell vacancy and an electron excited to an

empty state. It leads to different energies of the excitation with respect to the vacuum level in different spectra (due to different vacancies).²⁹ At the same time, we should emphasize that the energy separation between *a* and *b* (crystal-field splitting of the Ti 3*d* states into *t*_{2*g*} and *e*_g) remains almost unchanged in the spectra of fluorine and titanium: 2.37 eV (F 1*s* spectrum), 2.58 eV (Ti 2*p*_{3/2} spectrum), and 2.63 eV (Ti 2*p*_{1/2} spectrum).

The small widths of peaks *a* and *b* in both spectra indicate strong spatial localization of the *t*_{2*g*} and *e*_g excitations. From general principles and by analogy with the SF₆ and PF₆⁻ systems, it is natural to assume that these excitations are essentially localized at the central (Ti) atom and are primarily determined by the 3*dt*_{2*g*} and 3*de*_g states, which can be observed in the F 1*s* absorption spectrum of the TiF₆²⁻ anion due to covalent bonding between the Ti and F atoms. It should be noted here that the width (FWHM) of peaks *a* and *b* is different in the spectra compared: 0.37 eV (*a*) and 0.48 eV (*b*) in the Ti 2*p*_{3/2} spectrum; 0.99 eV (*a*) and 1.33 eV (*b*) in the F 1*s* spectrum. We are not comparing with the Ti 2*p*_{1/2} spectra, since there a strong Coster-Kronig decay of the Ti 2*p*_{1/2} hole contributes to the widths. Note that the ratios of the widths of peaks *a* and *b* are the same (3:4) in the spectra compared. These changes in the widths cannot be explained by differences in the energy resolution or in the core-hole lifetimes, since both spectra were taken with rather similar energy resolutions (115 meV for F 1*s*; 75 meV for Ti 2*p*); in addition, for both the F 1*s* and Ti 2*p*_{3/2} holes the lifetime widths are 0.2–0.3 eV.⁵ We therefore associate these findings with a smaller lifetime of the 3*de*_g and 3*dt*_{2*g*} excitations in the F 1*s* NEXAFS spectrum due to hopping of the excited electrons from the core-excited fluorine atom to neighboring fluorine atoms with no involvement of the core holes. The lifetime τ of these quasibound electronic states is determined by that of the core hole τ_h and that of the excited electron at the parent core-excited atom τ_e : $1/\tau = 1/\tau_h + 1/\tau_e$. The lifetime of the core hole is an intrinsic atomic property, which is only weakly affected by the surroundings in the solids, while τ_e is strongly influenced by the degree of localization of the excited electron. In the framework of a quasimolecular approach to the electronic structure of TM fluorides, the different values of τ_e for low-energy excitations (3*dt*_{2*g*} and 3*de*_g) at the Ti 2*p*_{3/2} and F 1*s* thresholds are caused by the different localization regions of the corresponding Ti and F excitations, which are primarily defined by the sizes of the Ti atom and the F octahedron, respectively. In other words, we assume that the solid-state environment will influence the x-ray absorption spectrum of the ligand atom (fluorine) of the molecular anion TiF₆²⁻ stronger than that of the central atom (titanium). We have previously observed a similar effect comparing NEXAFS and resonant photoemission spectra of the molecular anion NO₂⁻ in solid NaNO₂ at the N 1*s* and O 1*s* thresholds.³⁰ Finally, it should be also noted that the observed difference in the width of the Ti 2*p* and F 1*s* resonances can be partly caused by their different broadening due to the vibrational excitation of the TiF₆²⁻ quasimolecule in the process of x-ray absorption.

Thus the Ti 3*d* states in TiF₆²⁻ can be probed by F 1*s* NEXAFS. This conclusion is additionally supported by a comparative analysis of the F 1*s* spectra for octahedral SF₆,

PF₆⁻, and TiF₆²⁻. Indeed, when going from SF₆ and PF₆⁻ to TiF₆²⁻ one can clearly observe (i) a large shift of the absorption bands to lower energies (by ≈ 15 eV) related to the 3*d* states of the central atom (bands C and D for SF₆ and PF₆⁻ and peaks *a* and *b* for TiF₆²⁻) and (ii) a considerable decrease in their energy widths (see Fig. 3). These spectral changes are the result of a collapse and subsequent increase in localization of the 3*d* states of the central atom when going from atoms close to the end of the second row to atoms of the first TM series.³¹ This collapse of the 3*d* states manifests itself also in a strong decrease in the energy splitting of these states into *t*_{2*g*} and *e*_g components caused by the F octahedron: 13.6 eV (PF₆⁻), 13.3 eV (SF₆), and 2.37 eV (TiF₆²⁻). As noted above, in the framework of the crystal-field theory, this splitting is proportional to the quantities $\langle r^4 \rangle_{3d}$ and $R^{-5}(M-F)$.^{23–25} As a result of an increase in the interatomic distance $R(M-F)$ when going from PF₆⁻ (0.158 nm) and SF₆ (0.156 nm) (Ref. 18) to TiF₆²⁻ (0.192 nm),³² the crystal-field splitting in the case of TiF₆²⁻ should be reduced by a factor of 0.354, i.e., to a value of 4.71 eV as compared to 13.3 eV for SF₆. The splitting observed in the Ti 2*p*_{1/2,3/2} spectra of TiF₆²⁻ (2.63 and 2.58 eV) is about two times less than the expected one. Evidently, such an additional decrease in the 3*dt*_{2*g*}–3*de*_g splitting can only result from a strong contraction of the 3*d* wave functions due to the described collapse.³¹ Finally, we would like to note that the collapse of the 3*d* wave function is observed even more evidently in the 2*p* NEXAFS spectra of the central atoms when going from SF₆ to TiF₆²⁻.⁶

We turn again to Fig. 3 now in order to analyze one further interesting observation. As mentioned above, the intense absorption bands A and B in the spectra of SF₆ and PF₆⁻ are caused by the F 1*s* electron transitions to the lowest unoccupied electronic states of *a*_{1*g*} and *t*_{1*u*} symmetry. These states are described by MO's that, for these polyatomic systems, are made up of hybridized S(P) 3*s*+F 2*p* and S(P) 3*p*+F 2*p* character, respectively. Within the framework of our quasimolecular approach we assume that the corresponding absorption structures *c*–*e* in the second spectral region of the F 1*s* spectrum of TiF₆²⁻ reflect empty electronic states that result from the Ti 4*s*, 4*p*–F 2*p* covalent bonding (hybridization).

C. Comparison of the spectra of TiF₆²⁻ with those of TiO₂ and KF

In the preceding section we showed that the x-ray absorption spectra in the vicinity of core-electron thresholds reflect the quasimolecular character of the TiF₆²⁻ anion in solid K₂TiF₆. This means that NEXAFS excitations at the Ti 2*p* and F 1*s* thresholds of this crystalline compound occur mainly within the octahedron of fluorine atoms that is only scarcely affected by the rest of the solid. This allows us to give a unified interpretation of the Ti 2*p* and F 1*s* NEXAFS spectra of TiF₆²⁻, i.e., to associate the observed spectral features with the transitions of Ti 2*p* and F 1*s* electrons to the low-lying empty MO's of the covalent molecular anion. In the following, we shall show that the primary role of the fluorine octahedra for the NEXAFS spectra is also preserved

in ionic 3d TM fluorides, since in these compounds the TM atoms are also coordinated octahedrally or nearly octahedrally by fluorine atoms. Along with this similarity, however, there are important structural distinctions between K_2TiF_6 and 3d TM fluorides. First, the octahedral anions TiF_6^{2-} in K_2TiF_6 are quasi-isolated from each other, whereas in the ionic TM fluorides similar polyatomic MF_6 groups are linked together via their edges and corners forming a network of octahedra.¹⁸ Thus, in ionic TM fluorides, the x-ray absorption spectra of MF_6 are affected stronger by the crystal than in case of the quasi-isolated molecular anion TiF_6^{2-} . Second, the octahedra in 3d TM fluorides are usually considerably distorted causing changes in the F 1s NEXAFS spectra.

In order to clarify the effects of a linkage of the octahedra on the NEXAFS spectra of the central as well as the ligand atoms, we shall compare the absorption spectra of the quasi-isolated molecular anion TiF_6^{2-} in solid K_2TiF_6 with the spectra of rutile TiO_2 and KF. In rutile, the TiO_6 octahedra are linked in a three-dimensional network. We think that the electronic structure of rutile relevant to the NEXAFS spectra is mainly caused by the nearest-neighbor environment of the Ti atom, i.e., it is reasonable to compare TiF_6^{2-} in K_2TiF_6 with TiO_6 in TiO_2 ,³³ because these octahedral polyatomic groups (quasimolecules) are almost isostructural. Indeed, the oxygen octahedron around a given titanium atom is only slightly distorted in rutile, two Ti-O distances (0.199 nm) being slightly larger than the other four (0.194 nm).¹⁸ These distances are very close to the interatomic distance $R(Ti-F) = 0.192$ nm in K_2TiF_6 .³² Furthermore, absorption structures in molecular spectra result from multiple (resonance) scattering of low-energy photoelectrons in the molecular field,³⁴ and the differences in scattering properties of oxygen and fluorine atoms are small owing to their very similar electronegativities; they will therefore not contribute substantially to differences in the NEXAFS spectra of TiF_6^{2-} and TiO_2 . We suppose therefore that it is the octahedron linkage that is responsible for the main changes in absorption structures when going from TiF_6^{2-} to TiO_2 . In this case it appears natural that the greatest changes should be observed in the absorption spectra of the ligand atoms.

The x-ray absorption spectra of rutile have been measured repeatedly and have been discussed in Refs. 35–45. The spectra obtained in the present work (see Fig. 5) are better resolved [$\Delta E = 90$ meV (FWHM) in the case of the O 1s spectrum and 75 meV in the case of the Ti 2p spectrum] than most of the previously measured ones, but the overall spectral shape is in good agreement with the earlier studies. In Fig. 5, the Ti 2p and O 1s spectra were aligned in energy using the known energy separation (72.2 eV) between the Ti $2p_{3/2}$ and O 1s core levels in rutile.⁴⁶ It is clear from Fig. 5 that peaks *a* and *b* have about the same energy positions in the two spectra. As in the case of TiF_6^{2-} , they therefore reflect core-electron transitions in the oxygen and titanium atoms to the lowest unoccupied Ti $3d_{t_{2g}}$ and $3d_{e_g}$ electronic states that are hybridized with the 2p states of the ligand (oxygen) atoms. The bands *c*, *d*, and *e* in the O 1s spectrum are known to be related to the empty electronic states with mixed Ti 4s, $4p + O 2p$ character.^{35,37,39,41}

In the following, we shall compare the spectra of the central atom (Ti) and the ligand atoms (O and F) for TiO_2 and

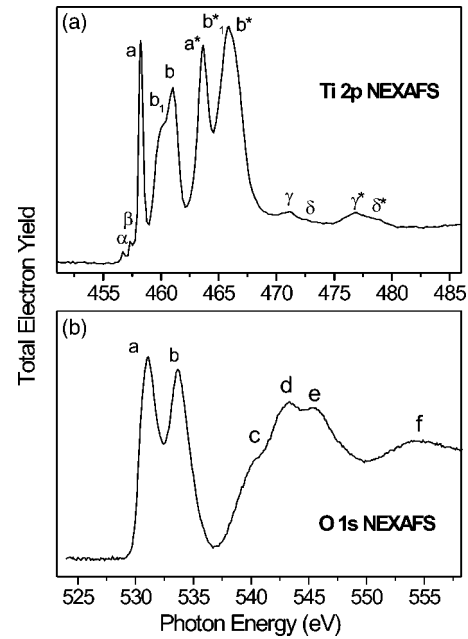


FIG. 5. Ti $2p_{1/2,3/2}$ (a) and O 1s (b) NEXAFS spectra of rutile TiO_2 . The Ti $2p_{1/2}$ structures were marked by asterisks. The spectra were aligned in energy by using the energy separation (72.2 eV) between the O 1s and Ti $2p_{3/2}$ core levels in rutile (Ref. 46).

TiF_6^{2-} . Figure 6 displays the Ti 2p absorption spectra of TiF_6^{2-} and TiO_2 recorded under identical experimental conditions. For the sake of convenience, the spectrum of rutile was shifted by ≈ 0.8 eV to higher photon energies in order to align the peaks *a* in the two spectra. The compared spectra have the same number of intense absorption bands (*a*, *b*, *a**, and *b**) and the weak peaks (α , β , γ , δ , γ^* , and δ^*) and have

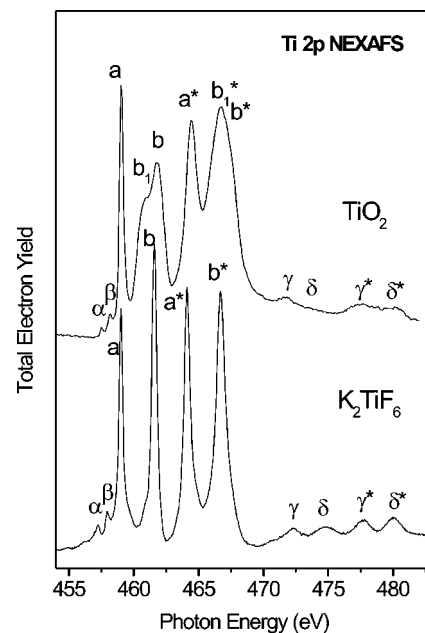


FIG. 6. Comparison between the Ti $2p_{1/2,3/2}$ NEXAFS spectra of the molecular anion TiF_6^{2-} in solid K_2TiF_6 and in the rutile TiO_2 . The spectrum of TiO_2 was aligned in energy with that of TiF_6^{2-} at the position of the first absorption peak *a*.

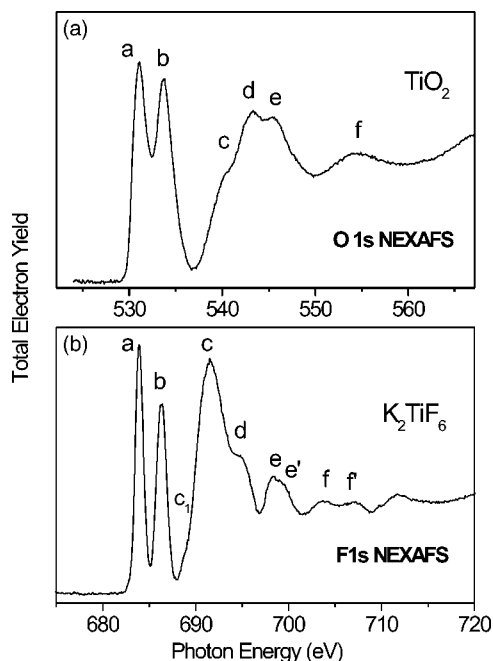


FIG. 7. Comparison of the O 1s NEXAFS spectrum of rutile TiO₂ (a) with the F 1s spectrum of the molecular anion TiF₆²⁻ in solid K₂TiF₆ (b). The spectrum of TiO₂ was aligned in energy with that of TiF₆²⁻ at the position of the first absorption peak *a*.

similar line shapes. The biggest differences between these spectra are given by in the widths of the absorption bands *b*, *a*^{*}, and *b*^{*} that are essentially broader in the spectrum of rutile. On the other hand, the increase of the width of peak *a* is insignificant. For bands *b* and *b*^{*}, the shape changes are particularly strong: these bands split into two bands *b*₁-*b* and *b*₁^{*}-*b*^{*} in the spectrum of TiO₂. This doubling of the Ti 2_p-3*d*_g transitions in case of TiO₂ is well known and has been discussed repeatedly in the past.^{39,41,45} As a result, there are three different explanations for the origin of this effect: (i) a transformation of the *e*_g MO's of the MO₆ groups into an *e*_g band in the crystal;³⁹ (ii) a splitting of the 3*d*_g component due to the dynamic Jahn-Teller effect;³⁹ (iii) a reduction of the real site symmetry of Ti in rutile from *O*_h to *D*_{4h} or *D*_{2h}.⁴¹ On the other hand, a theoretical analysis claims that the distortions of the *O*_h symmetry cannot explain this doubling of the Ti 2_p→3*d*_g transitions in case of TiO₂,⁴⁵ which would mean that the above explanations might be incorrect.

The ligand 1s absorption spectra (oxygen and fluorine) of TiF₆²⁻ and TiO₂ are presented in Fig. 7; they are aligned in energy at the position of peak *a*. It is very striking that the ligand spectra show a closer similarity than the spectra of the central (Ti) atom. We observe only a broadening of peaks *a* and *b* that are associated with the Ti 3*d*_{2g} and 3*d*_g electronic states, furthermore, small shifts of bands *c* and *d* to higher energies, and differences in the relative intensity of bands *c*, *d*, and *e*. The latter bands reflect core-electron transitions to the unoccupied 4*s**a*_{1g} and 4*p**t*_{1u} electronic states of the Ti atom hybridized with the 2*p* states of the ligand atoms (oxygen or fluorine). These changes cannot be related to a difference in energy resolution, since the O 1s and F 1s NEXAFS spectra were recorded with quite similar energy

resolutions of 90 and 115 meV, respectively. Apart from the above spectral differences, a certain similarity between the low-energy absorption structures in the spectra of TiO₂ and TiF₆²⁻ is obvious.

This allows us to consider the absorption structures in the two spectra of rutile in a similar way, as discussed above for the case of TiF₆²⁻, i.e., within a quasimolecular approach. To this end, we assign these structures to core-electron transitions to the lowest unoccupied MO's of the octahedral TiO₆ quasimolecule, despite the linkage of these octahedra in rutile. In this case, the octahedron linkage should be treated as only a weak perturbation that causes mainly an additional delocalization of the final (excited) states and, as a consequence, a broadening of the corresponding spectral features. This perturbation will not change the character of the final states, i.e., it will preserve their quasimolecular nature that is formed by the TiO₆ quasimolecule.

A more detailed consideration of the rutile structure allows us to make one further suggestion: In the rutile structure there are two types of TiO₆ octahedra with different orientations,¹⁸ which are joined together via two opposite edges to form a chain. The chains are linked by common corners and form an octahedral network. The 3*d*_g orbitals are directed towards the corners of the octahedra (oxygen anions), which means that they should be more sensitive to changes in the chemical state of the oxygen atoms as compared to the 3*d*_{2g} orbitals that are oriented towards the edges of the octahedra. On this basis we suppose that the presence of two orientations of the TiO₆ octahedra in rutile is responsible for the observed doubling of the 3*d*_g spectral features in the Ti 2*p* NEXAFS spectrum, whereas the octahedra linkage is expected to cause only a broadening of the absorption structures. Besides that, some broadening of the absorption bands in the spectra of TiO₂ originates from small distortions of the TiO₆ octahedron. Because of the Ti 3*d*-O 2*p* hybridization, one could expect that the splitting of the 3*d*_g states should also be reflected in the O 1s absorption spectrum as a splitting of peak *b*. However, this splitting is hidden due to the large broadening of the low-energy absorption bands *a* and *b* that is comparable to the full width of the doubled 3*d*_g component in the Ti 2*p* spectrum (see Fig. 5). It should be noted here that a similar doubling of the 3*d*_g component has not been observed in the Ti 2*p* x-ray absorption spectra of FeTiO₃ (Ref. 41) and SrTiO₃ (Ref. 47) that contain TiO₆ octahedra with the same orientation. A more detailed comparative analysis of the absorption spectra of TiO₂ and TiF₆²⁻, including consideration of the low-intensity structures *α*, *β*, *γ*, *δ*, will be given elsewhere.

Thus, by comparing K₂TiF₆ with TiO₂, we have shown that the fluorine (oxygen) octahedron around the central Ti atom plays a decisive role in the formation of the spectral features at low energies in the F (O) 1s NEXAFS spectra of these compounds, while the interoctahedral interaction is of less importance. In order to demonstrate that this rule is more general and can be applied to compounds with different types of interoctahedral linkage, we now compare the fluorine spectra of the quasimolecular anion TiF₆²⁻ and of the "classical" ionic crystal KF (see Fig. 8). The latter can be considered to be composed of a network of nondistorted KF₆ octahedra joined by all sharing edges.¹⁸ The spectra consid-

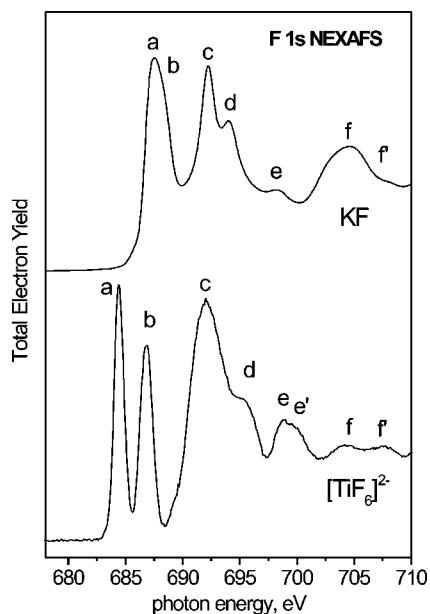


FIG. 8. F 1s NEXAFS spectra of the ionic crystal KF and of the molecular anion TiF_6^{2-} in solid K_2TiF_6 .

ered are clearly similar in line shape and are characterized by two low-energy peaks *a* and *b* (unresolved in case of KF) as well as by well-defined structures *c*, *d*, and *e* close to the F 1s absorption threshold (at ≈ 690 eV). In Fig. 9, the K 2*p* x-ray absorption spectrum, recorded with 50-meV energy resolution, is aligned in energy with the F 1s spectrum of KF making use of the known energy separation between

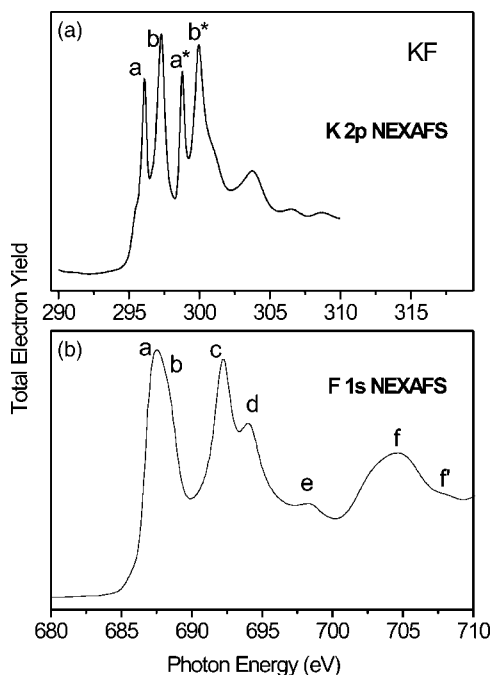


FIG. 9. K 2*p*_{1/2,3/2} (a) and F 1s (b) NEXAFS spectra of ionic KF. The K 2*p*_{1/2} structures were marked by asterisks. The spectra were aligned in energy using the energy separation (390.55 eV) between the F 1s and K 2*p*_{3/2} core levels in KF, measured by photoemission.

the F 1s and K 2*p*_{3/2} core levels (390.55 eV) measured by photoemission. It is clearly seen that the low-energy structures in the fluorine spectrum of KF have very similar energy positions as the analogous spectral features in the K 2*p*_{3/2} x-ray absorption spectrum, i.e., stemming from transition to the unoccupied 3*dt*_{2g} and 3*de*_g states. This allows us to assume a common origin of the lower-energy absorption peaks in the two spectra of KF, i.e., the 3*dt*_{2g} and 3*de*_g states of the central K atom, split by the field of the fluorine octahedron that must have a mixed K 3*d*+F 2*p* character in order to contribute to both NEXAFS spectra.

The energy spacing 3*dt*_{2g}-3*de*_g is the same (1.18 eV) in the K 2*p*_{3/2} and 2*p*_{1/2} spectra within the experimental accuracy. The shape of the low-energy absorption band *a*-*b* in the F 1s spectrum agrees also well with the assumption that it consists of two unresolved components separated by an energy spacing of ≈ 1.2 eV. This 3*dt*_{2g}-3*de*_g splitting, which is about two times smaller than that in TiF_6^{2-} (2.37 eV in the F 1s spectrum), should be associated with the increase of the interatomic distance between central and ligand atoms when going from the TiF_6^{2-} (0.192 nm) to the KF_6 octahedron [0.266 nm (Ref. 18)]. However, according to the above-mentioned expression $10Dq=5eq\langle r^4 \rangle_{3d}/3R^5$ for the crystal-field splitting,²³⁻²⁵ this large change in the octahedron size must cause a stronger decrease of the 3*d* splitting, namely from 2.37 to 0.46 eV, if the average radii $\langle r \rangle_{3d}$ of the K and Ti 3*d* wave functions in KF and TiF_6^{2-} are equal to each other. The discrepancy between this predicted splitting and the value observed experimentally (≈ 1.2 eV) results probably from a larger radius of the 3*d* wave function of the K⁺ cation due to an incomplete collapse in comparison with the titanium cation.^{31,48} It should also be noted that the empty cation 3*d* states have different energy positions with respect to the onset of the F 1s continuum (at ~ 688 eV) in the fluorine spectra of KF and TiF_6^{2-} indicating an incomplete collapse of the 3*d* wave function for K⁺. Finally, we should emphasize that we have observed and discussed the collapse of the 3*d* electronic states along the P-S-K-Ti series in PF_6^- , SF_6 , KF, and TiF_6^{2-} indirectly via the F 1s absorption spectra. Contrary to the observation of a collapse in the cation x-ray absorption spectra,⁴⁸ our present findings demonstrate a “pure” 3*d* collapse for the electronic configurations without 2*p* core holes on the cation sites. In this regard our measurements are similar to a study by inverse photoemission that probes empty atomiclike electronic states without the creation of a deep core hole that will perturb the ground state of the atom under consideration.⁴⁹ Evidently, the present observation of a 3*d* collapse in the F 1s NEXAFS spectra is the result of strong covalent mixing between the cation 3*d* and fluorine 2*p* electronic states in PF_6^- , SF_6 , KF, and TiF_6^{2-} .

D. Consideration of the F 1s absorption spectra for 3*d* TM fluorides

We now discuss the role of covalent bonding in the formation of the unoccupied electronic states in going from purely covalent reference systems to rather ionic binary fluorides. Note that all 3*d* TM fluorides studied possess an octahedral or nearly octahedral fluorine environment of the 3*d*

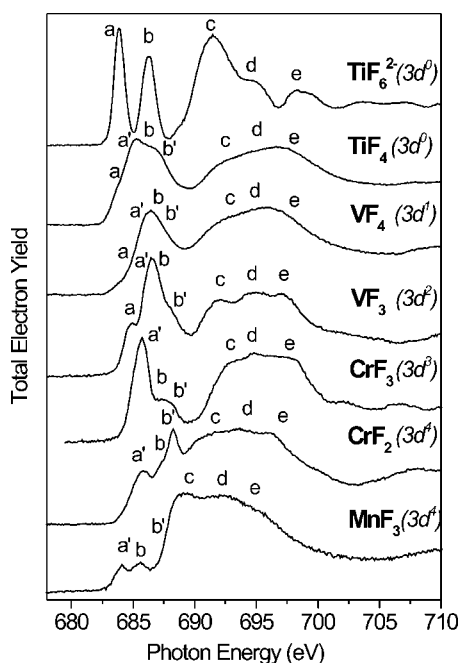


FIG. 10. High-resolution F 1s NEXAFS spectra of the 3d TM fluorides K_2TiF_6 , TiF_4 , VF_4 , VF_3 , CrF_3 , CrF_2 , and MnF_3 recorded in the photon-energy range from 678 to 710 eV. The formal 3d electron configuration of the TM atoms is given in parentheses.

TM atoms.¹⁸ The TM difluorides studied possess the rutile structure, whereas the crystal structure of the trifluorides is similar to that of ReO_3 , where oxygen (fluorine) octahedra are linked via their corners. The crystal structure of the tetrafluorides of the 3d TM atoms, TiF_4 and VF_4 , can be described by arrays of layers of MF_6 octahedra with a considerable tetragonal (C_{4v}) distortion linked by four shared equatorial corners.¹⁸ Based on the localized and oriented character of covalent bonds and taking into account the results of the preceding discussion, we assume that one can consider the octahedral quasimolecules MF_6 formed by the 3d TM atom and the surrounding fluorine atoms as the main building blocks of the crystalline material not only in rather covalent 3d systems, but also in ionic TM fluorides. This quasimolecular approach is an elegant way to gain deep qualitative insight into the nature of chemical bonding in these classical solids. In particular, it implies that the above results obtained for the covalent molecular TiF_6^{2-} anion, the covalent TiO_2 crystal, and the classical ionic KF crystal can be quite useful for the analysis of spectra of binary ionic fluorides.

We now consider in more detail the low-energy structures in the F 1s x-ray absorption spectra (Figs. 10 and 11). The similarity of overall line shapes and energy positions for these structures in the spectra of the ionic fluorides and the covalent molecular anion TiF_6^{2-} allows us to assign them in both cases to unoccupied electronic states with mixed TM 3d–F 2p character that results from a significant covalent bonding between the valence electrons of the central TM atom and the surrounding fluorine atoms. However, when going from the TiF_6^{2-} anion to the binary fluorides and further along the series $TiF_4 \cdots ZnF_2$, the spectra in Figs. 10

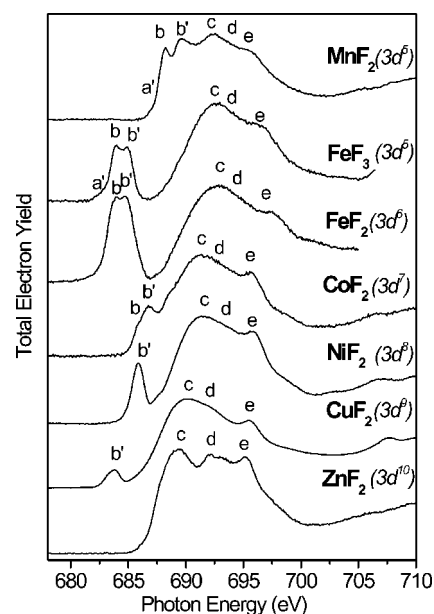


FIG. 11. High-resolution F 1s NEXAFS spectra of the 3d TM fluorides MnF_2 , FeF_3 , FeF_2 , CoF_2 , NiF_2 , CuF_2 , and ZnF_2 recorded in the photon-energy range from 678 to 710 eV. The formal 3d electron configuration of the TM atoms is given in parentheses.

and 11 exhibit substantial changes in the number and relative intensities of the resonances, as well as in their energy positions with respect to each other and to the onset of the F 1s continuum, which is found in all spectra to be close to 687–688 eV. These changes are likely caused by: (i) the decreasing number of the unoccupied 3d states of the TM atom accompanied by an increasing localization of these states along the series; (ii) different exchange interactions between the 3d electrons in partially filled shells; (iii) variations in magnitude and character of the distortion of the fluorine octahedron; and (iv) different influences of the remaining parts of the solid on the quasimolecule MF_6 . The latter, in particular, will lead to a different coupling between these quasimolecular units in the crystal. Therefore a complete understanding of all these changes might only be possible on the basis of detailed calculations of the F 1s NEXAFS spectra of the binary fluorides, which have not been reported in the literature so far.

Despite this, we can make some assumptions about the origin of the observed low-energy structures in the NEXAFS spectra. Taking into account the results of our comparative quasimolecular analysis of the NEXAFS spectra of TiF_6^{2-} , TiO_2 , and KF, we can first suppose that the linkage between the MF_6 octahedra in the TM fluorides has only a minor influence on the shapes of the absorption features in the F 1s spectra. Calculations of the electronic structures of 3d TM oxides⁵⁰ show that consideration of the exchange interaction between the 3d electrons leads to an additional splitting of the $3dt_{2g}$ and $3de_g$ electronic states of MO_6 into $t_{2g}\uparrow$, $e_g\uparrow$, $t_{2g}\downarrow$, and $e_g\downarrow$ components related to two possible spin orientations: spin up (\uparrow) or spin down (\downarrow), respectively. Evidently, a similar situation must hold for MF_6 in the 3d TM fluorides. It is also clear that the ordering of these split 3d

components depends on the ratio between the magnitudes of the crystal-field and exchange splittings. The following discussion will allow us to suppose that the crystal-field splitting is larger than the exchange splitting, which—in turn—leads to an ordering of the $3d$ components $t_{2g}\uparrow$, $t_{2g}\downarrow$, $e_g\uparrow$, and $e_g\downarrow$.

Based on the formal valence, one may assume that titanium (with a $3d^24s^2$ valence-electron atomic configuration) has the same electronic configuration of the Ti^{4+} ion in the molecular anion TiF_6^{2-} and in solid TiF_4 , with no $3d$ electrons. In this case, the $3d$ - $3d$ exchange interaction is absent and the peaks a and b in the spectrum of TiF_6^{2-} can be related to electronic transitions to the $3dt_{2g}$ and $3de_g$ states that are not split by exchange interaction. Therefore the variations of the low-energy absorption structures when going from TiF_6^{2-} to TiF_4 result from a considerable tetragonal (C_{4v}) distortion of the TiF_6 octahedra in the titanium fluorides. The latter causes: (i) splittings of the absorption bands a ($3dt_{2g}$ component) and b ($3de_g$ component) into two subbands $a-a'$ ($3de$ and $3db_2$ components) and $b-b'$ ($3da_1$ and $3db_1$ components), respectively;^{23–25} (ii) a merging of the two low-energy absorption bands a and b into one broad band $a-a'-b-b'$.

In contrast to the situation in other binary fluorides (of vanadium, chromium, etc.), these states are additionally split due to exchange interaction between the $3d$ electrons. The $3d$ electrons occupy successively the $t_{2g}\uparrow$, $t_{2g}\downarrow$, $e_g\uparrow$, and $e_g\downarrow$ states according to their statistical weights that are 3 and 2 for t_{2g} and e_g components, respectively.

In VF_4 one available $3d$ electron of the V^{4+} cation partly fills the lowest $3dt_{2g}\uparrow$ band that can be additionally split into two components by a considerable distortion of the F_6 -derived octahedron, as observed in the case of TiF_4 . As a consequence, one broad band $a-a'-b-b'$ is observed in the low-energy part of the F $1s$ NEXAFS spectrum of VF_4 . It is clearly seen that the exchange interaction between the $3d$ electron and the excited electron does not contribute substantially to an additional broadening of the low-energy absorption band $a-a'-b-b'$.

The formal valence configuration $3d^2$ of the vanadium ion V^{3+} in VF_3 , with a nearly perfect VF_6 octahedron, indicates that the corresponding F $1s$ NEXAFS spectrum might exhibit all four exchange-split $3d$ components, since the lowest $t_{2g}\uparrow$ state will not remain fully occupied. Due to the almost perfect octahedral shape of VF_6 , the absorption spectrum of VF_3 reveals sharper features than the spectra of VF_4 and TiF_4 . The overall shape of its low-energy structure $a-a'-b'$ does not rule out the existence of an additional unresolved component b in the region of the broad peak a' . Note that the crystal-field splitting of VF_3 , with an interatomic distance of $R(V-F)=0.195$ nm,¹⁸ is probably not much different from that (2.37 eV) of TiF_6^{2-} , with $R(Ti-F)=0.192$ nm. As seen in Fig. 10, this estimate is in agreement with the line shape of the low-energy absorption structures.

In case of the chromium fluorides, CrF_3 and CrF_2 , the lowest $t_{2g}\uparrow$ state is already completely filled. Therefore only three low-energy features a' , b , and b' (related to a transition to the $t_{2g}\downarrow$, $e_g\uparrow$, and $e_g\downarrow$ states, respectively) are observed in the spectra. The dramatic changes in the relative intensities of these absorption structures in CrF_2 as compared to CrF_3

can be associated with the large distortion of the CrF_6 octahedron caused by a strong Jahn-Teller effect.¹⁸

The $t_{2g}\downarrow$ state gets gradually occupied when going from $CrF_3(3d^3)$ to CrF_2 , $MnF_3(3d^4)$, MnF_2 and $FeF_3(3d^5)$. As a result, the intensity of the first absorption structure, a' , decreases gradually. Similarly, only two transitions to the $e_g\uparrow$ and $e_g\downarrow$ states are observed in the spectra of FeF_2 and CoF_2 , since the $e_g\uparrow$ state in these compounds is filled. For NiF_2 and CuF_2 , where solely one unoccupied electronic state $e_g\downarrow$ remains, only one absorption peak b' is observed in the low-energy part of the F $1s$ NEXAFS spectra. In the spectrum of ZnF_2 , the low-energy structure is absent since all $3d$ states are filled in this compound.

In summarizing the results of our analysis of the low-energy structures in the F $1s$ NEXAFS spectra, we note that the conclusion concerning covalent contributions to chemical bonding in the TM fluorides can already be obtained on the basis of the mere observation of the F $1s$ spectra. Indeed, within a simple ionic description, the lowest conduction band of these compounds should successively be formed from the empty $3d$, $4s$, and $4p$ states of the TM cation, whereas the fully occupied F $2p$ states should constitute the top of the valence band. The absence of unoccupied F $2p$ states would then prevent any strong $1s \rightarrow 2p$ dipole transitions, in contrast to our observations. Allowed dipole transitions of F $1s$ electrons to the delocalized $3p$ states are located in the continuum far above the ionization threshold and should have very low intensities. Therefore they cannot noticeably contribute to the F $1s$ NEXAFS spectra. As a result, we conclude that the F $1s$ NEXAFS spectra in the region between 690 and 700 eV reflect electron transitions to unoccupied states formed mainly by covalent mixing of the $4s$ and $4p$ states of the TM atom with the $2p$ states of the F atom.

In conclusion, we emphasize that the basic results of this work provide strong experimental evidence for the important role of covalent mixing in the formation of the unoccupied electronic states in crystalline $3d$ TM fluorides. The F $1s$ NEXAFS spectra are found to be well suited for probing the unoccupied $3d$ states of the (TM) atoms in these compounds. The present results are in good agreement with the conclusions of similar studies of TM compounds with less ionic character, as, e.g., the $3d$ TM oxides.^{35–37,40,51,52}

ACKNOWLEDGMENTS

This work was supported by the Russian Foundation for Basic Research (Project Nos. 01-03-32285, 04-02-17216, and 04-02-17646), the Deutsche Forschungsgemeinschaft (Grant Nos. SFB 463, TP B4, and B16), the Freie Universität Berlin, and the bilateral Program “Russian-German Laboratory at BESSY.” We thank the staff of BESSY for valuable technical assistance. A. S. Vinogradov, S. I. Fedoseenko, and V. N. Sivkov gratefully acknowledge financial support from BESSY and from the Technische Universität Dresden. A. B. Preobrajenski acknowledges support from the Swedish Foundation for International Cooperation in Research and Higher Education (STINT).

- *Corresponding author: Fax +7-812-428-7240; email address: Alexander.Vinogradov@pobox.spbu.ru
- ¹J. Zaanen, G. A. Sawatzky, and J. W. Allen, *Phys. Rev. Lett.* **55**, 418 (1985).
 - ²S. A. Gorovikov, S. L. Molodtsov, and R. Follath, *Nucl. Instrum. Methods Phys. Res. A* **411**, 506 (1998).
 - ³S. A. Gorovikov, R. Follath, S. L. Molodtsov, and G. Kaindl, *Nucl. Instrum. Methods Phys. Res. A* **467–468**, 565 (2001).
 - ⁴S. I. Fedoseenko, I. E. Iossifov, S. A. Gorovikov, J.-H. Schmidt, R. Follath, S. L. Molodtsov, V. K. Adamchuk, and G. Kaindl, *Nucl. Instrum. Methods Phys. Res. A* **470**, 84 (2001).
 - ⁵K. C. Prince, M. Vondráček, J. Karvonen, M. Coreno, R. Camilioni, L. Avaldi, and M. de Simone, *J. Electron Spectrosc. Relat. Phenom.* **101–103**, 141 (1999).
 - ⁶A. S. Vinogradov, A. Yu. Dukhnyakov, V. M. Ipatov, D. E. Onopko, A. A. Pavlychev, and S. A. Titov, *Fiz. Tverd. Tela (S.-Peterburg)* **24**, 1417 (1982) [*Sov. Phys. Solid State* **24**, 803 (1982)].
 - ⁷S. Nakai, A. Kawata, M. Ohashi, M. Kitamura, C. Sugiura, T. Mitsuishi, and H. Maezawa, *Phys. Rev. B* **37**, 10 895 (1988).
 - ⁸M. Umeda, Y. Tezuka, S. Shin, and A. Yagishita, *Phys. Rev. B* **53**, 1783 (1996).
 - ⁹A. S. Vinogradov, A. Yu. Dukhnyakov, T. M. Zimkina, V. M. Ipatov, I. V. Karunina, D. E. Onopko, A. A. Pavlychev, S. A. Titov, and E. O. Filatova, *Fiz. Tverd. Tela (S.-Peterburg)* **22**, 2602 (1980) [*Sov. Phys. Solid State* **22**, 1517 (1980)].
 - ¹⁰A. S. Vinogradov, T. M. Zimkina, and V. A. Fomichev, *Zh. Strukt. Khim.* **12**, 899 (1971). [*J. Struct. Chem.* **12**, 823 (1971)].
 - ¹¹T. M. Zimkina and A. S. Vinogradov, *J. Phys. (Paris), Colloq.* **32**, C4-3 (1971).
 - ¹²J. L. Dehmer, *J. Chem. Phys.* **56**, 4496 (1972).
 - ¹³E. Hudson, D. A. Shirley, M. Domke, G. Remmers, A. Pushman, T. Mandel, C. Xue, and G. Kaindl, *Phys. Rev. A* **47**, 361 (1993).
 - ¹⁴J. T. Francis, C. C. Turci, T. Tyliczszak, G. G. B. de Souza, N. Kosugi, and A. P. Hitchcock, *Phys. Rev. A* **52**, 4665 (1995).
 - ¹⁵S. Nakai, M. Ohashi, T. Mitsuishi, H. Maezawa, H. Oizumi, and T. Fujikawa, *J. Phys. Soc. Jpn.* **55**, 2436 (1986).
 - ¹⁶E. Hudson, E. Moler, Y. Zheng, S. Kellar, P. Heimann, Z. Husain, and D. A. Shirley, *Phys. Rev. B* **49**, 3701 (1994).
 - ¹⁷A. S. Vinogradov, S. I. Fedoseenko, D. V. Vyalikh, S. L. Molodtsov, V. K. Adamchuk, C. Laubschat, and G. Kaindl, *Opt. Spektrosk.* **93**, 935 (2002) [*Opt. Spectrosc.* **93**, 862 (2002)].
 - ¹⁸A. Wells, *Structural Inorganic Chemistry*, 5th ed. (Oxford University Press, Oxford, UK, 1984).
 - ¹⁹J. L. Dehmer and D. Dill, in *Proceedings of Symposium on Electron-Molecule Collisions*, edited by I. Shimamura and M. Matsuzawa (University of Tokyo, Tokyo, 1979), p. 95.
 - ²⁰J.-H. Fock, Ph.D. dissertation, Universität Hamburg, 1983.
 - ²¹A. S. Vinogradov, V. N. Akimov, T. M. Zimkina, and A. A. Pavlychev, *Izv. Ross. Akad. Nauk, Ser. Fiz.* **49**, 1458 (1985) [*Bull. Acad. Sci. USSR, Phys. Ser. (Engl. Transl.)* **49**, 1 (1985)].
 - ²²A. A. Bakke, H.-W. Chen, and W. L. Jolly, *J. Electron Spectrosc. Relat. Phenom.* **20**, 333 (1980).
 - ²³C. J. Ballhausen, *Introduction to Ligand Field Theory* (McGraw-Hill, New York, 1962).
 - ²⁴S. Sugano, Y. Tanabe, and H. Kamimura, *Multiplets of Transition-Metal Ions in Crystals* (Academic, New York, 1970).
 - ²⁵I. B. Bersuker, *Electronic Structure and Properties of Coordination Compounds*, 2nd ed. (Khimiya, Leningrad, 1976).
 - ²⁶U. Fano and J. W. Cooper, *Rev. Mod. Phys.* **40**, 441 (1968).
 - ²⁷H. Ebert, J. Stöhr, S. S. P. Parkin, M. Samant, and A. Nilsson, *Phys. Rev. B* **53**, 16 067 (1996).
 - ²⁸B. Wallbank, J. S. H. Q. Perera, D. C. Frost, and C. A. McDowell, *J. Chem. Phys.* **69**, 5405 (1978).
 - ²⁹*Unoccupied Electronic States: Fundamentals for XANES, EELS, IPS, and BIS*, edited by J. C. Fuggle and J. E. Inglesfield (Springer, Berlin, 1992).
 - ³⁰A. S. Vinogradov, A. B. Preobrajenski, S. L. Molodtsov, S. A. Krasnikov, R. Szargan, A. Knop-Gericke, and M. Hävecker, *Chem. Phys.* **249**, 249 (1999).
 - ³¹R. I. Karaziya, *Usp. Fiz. Nauk* **135**, 79 (1981) [*Sov. Phys. Usp.* **24**, 775 (1981)].
 - ³²J. A. Ibers and C. H. Holm, *Acta Crystallogr.* **10**, 139 (1957).
 - ³³Taking into account the linkage character of the TiO₆ octahedra in this crystal (Ref. 18) and formal valencies of the titanium and oxygen atoms (4 and 2, respectively), the formal total charge of the TiO₆ octahedron in rutile reduces to zero.
 - ³⁴J. Stöhr, *NEXAFS Spectroscopy* (Springer, Berlin, 1992).
 - ³⁵L. A. Grunes, R. D. Leapman, C. N. Wilker, R. Hoffman, and A. B. Kunz, *Phys. Rev. B* **25**, 7157 (1982).
 - ³⁶R. D. Leapman, L. A. Grunes, and P. L. Fejes, *Phys. Rev. B* **26**, 614 (1982).
 - ³⁷A. S. Vinogradov, A. Yu. Dukhnyakov, V. M. Ipatov, A. A. Pavlychev, and V. N. Sivkov, *Fiz. Tverd. Tela (S.-Peterburg)* **25**, 400 (1983) [*Sov. Phys. Solid State* **25**, 225 (1983)].
 - ³⁸R. Brydson, B. G. Williams, W. Engel, H. Sauer, E. Zeitler, and J. M. Thomas, *Solid State Commun.* **64**, 609 (1987).
 - ³⁹R. Brydson, H. Sauer, W. Engel, J. M. Thomas, E. Zeitler, N. Kosugi, and H. Kuroda, *J. Phys.: Condens. Matter* **1**, 797 (1989).
 - ⁴⁰F. M. F. de Groot, M. Grioni, J. C. Fuggle, J. Ghijsen, G. A. Sawatzky, and H. Petersen, *Phys. Rev. B* **40**, 5715 (1989).
 - ⁴¹F. M. F. de Groot, J. C. Fuggle, B. T. Thole, and G. A. Sawatzky, *Phys. Rev. B* **41**, 928 (1990).
 - ⁴²G. van der Laan, *Phys. Rev. B* **41**, 12 366 (1990).
 - ⁴³R. Brydson, H. Sauer, W. Engel, and F. Hofer, *J. Phys.: Condens. Matter* **4**, 3429 (1992).
 - ⁴⁴F. M. F. de Groot, J. Faber, J. J. M. Michiels, M. T. Czyżyk, M. Abbate, and J. C. Fuggle, *Phys. Rev. B* **48**, 2074 (1993).
 - ⁴⁵J. P. Crocombette and F. Jollet, *J. Phys.: Condens. Matter* **6**, 10 811 (1994).
 - ⁴⁶L. Ramqvist, K. Hamrin, G. Johansson, A. Fahlman, and C. Nordling, *J. Phys. Chem. Solids* **30**, 1835 (1969).
 - ⁴⁷C. Schüßler-Langenheine, M. Haverkort, Z. Hu, M. Braden, L. H. Tjeng, E. Schierle, A. Starodubov, G. Kaindl, E. Weschke, G. Rijnders, M. Huijben, and D. H. A. Blank, *BESSY Annual Report 2002*, p. 162.
 - ⁴⁸A. A. Maiste, R. E. Ruus, and M. A. Elango, *Zh. Eksp. Teor. Fiz.* **79**, 1671 (1980) [*Sov. Phys. JETP* **52**, 844 (1980)].
 - ⁴⁹S. L. Molodtsov, C. Laubschat, and G. Kaindl, *Phys. Rev. B* **49**, 17 472 (1994).
 - ⁵⁰C. Suzuki, J. Kawai, H. Adachi, and T. Mukoyama, *Chem. Phys.* **247**, 453 (1999).
 - ⁵¹L. A. Grunes, *Phys. Rev. B* **27**, 2111 (1983).
 - ⁵²F. M. F. de Groot, *Chem. Rev. (Washington, D.C.)* **101**, 1779 (2001).